The Effects of Chemical Oxidation on Corrosion Behavior of Ni-Ti Alloy

The Effects of Chemical Oxidation on Corrosion Behavior of Ni-Ti Alloy

Nawal Mohammed Dawood and Enass L Ali

College of Materials Engineering, University of Babylon, Iraq

E-mail: mat.newal.mohammed@uobabylon.edu.iq

Abstract. Nickel Titanium intermetallic (NiTi) has been used in several fields (mostly corrosion issues were not a concern) since it was discovered about sixteen years ago. In the last decade, alloys made from NiTi have been widely used in the internal and external biomedical tools and equipment such as nails, fixation plates, bone fracture, self-expanding cardiovascular and urological stents, and orthodontic wires. The effects of chemical oxidation on corrosion behavior of Nickel-Titanium shape memory alloy have been investigated in this study. Technique of powder metallurgy was used to prepare the alloy from the elemental powders of Titanium and Nickel with 600 MPa of compacting pressure. The sintering process was achieved in a 10^{-4} torr vacuum atmosphere at 950 ˚C . XRD analysis exhibited that Ni and Ti were fully transformed into NiTi (both monoclinic and cubic phase) and Ni_3Ti phase. After sintering, the samples are grinded and polished, then samples were surface modified by chemical oxidation. Optical microscopy, scanning and x-ray diffraction techniques were utilized for characterizing the surface samples. The corrosion rate has been studied in vitro by using polarization curves technique in NaF solution at different concentration (0.5, 1,1.5, 2) wt ,%. Results of corrosion test indicated that the corrosion current density after chemical oxidation decreased from 0.303 for bare sample to 0.074 in 0.5% NaF solution, which indicates that TiO_2 layer on the NiTi SMA surface are protective after chemical oxidation.
Keywords. Nickel titanium alloys, Chemical oxidation, Corrosion resistance.

1. Introduction

Shape memory alloys (SMAs) have been well known due to their ability in memorizing and recovering their original shape exactly after deformation. SMAs existed in two various temperature-dependent crystal structures (phases). The phase at lower temperature is called martensite, while the phase at higher temperature is called austenite. SMAs can fully recover strains up to 8% [1,2] as they deform by twinning process mechanism instead of the conventional dislocation slip one. This happens due to the diffusionless and thermoelastic transformation of martenstic phase within the SMAs structure. Two separate mechanical effects characterize the response of shape memory alloys; pseudoelasticity and strain-memory effect. In pseudoelasticity or superelasticity, martensite reverts to the austenite phase upon unloading without heating. On the other hand, strain-memory effect requires heating to recover the martensite to the austenite phase because the deformation is irreversible. Strain memory effect can also be thermally induced, in this case, the structure consists of thermally induced martensite [3]. NiTi are the most important group of SMAs. The chemical composition of NiTi SMAs ranged from 53wt%-57 wt% nickel balance titanium [3,4]. There are many commercial applications of NiTi SMAs. These alloys exhibit strong shape memory effect and pseudoelastic behavior, which are

absolutely new properties when compared with the alloys made from conventional metals. These new properties make these materials perfect to be used for different applications. Moreover, the SMAs exhibit high corrosion resistance and biocompatible as well, making them appropriate for use in various fields of biomedical applications such as cardiovascular, orthodontics, orthopedics and neurosurgery applications [5,6]. Currently, NiTi SMAs production having a porous characteristic has drawn significant attention owing to their extraordinary mechanical characteristics along with the porous structures that are analogous to those of some natural biomaterials used in hard tissue implants. The bonding strength increased when the material has porous nature as the existing bone tissue can migrate inwards the bone. Additionally, the properties of the implant can be engineered to meet the properties of the bone [7]. The main concern of using Nitinol medical application is the dissolution of free nickel ions which are toxic and may even cause carcinogenic effects. This harmful metal release can preclude an appropriate surface modification [8]. Nitinol corrosion resistance is principally affected by its chemical surface conditions. Ti is very active element and when Nitinol is in contact with even a weak oxidizing environment with Nitinol, a very thin native passive layer predominated by titanium dioxide forms on the surface of Nitinol. There are many surface treatments aiming to improve the properties of this surface passive layer. These treatments result in an improvement in the corrosion resistance. Additionally, reducing the Ni content within the surface oxide layer is helpful as this reduction leads to decreasing the nickel ion releasing rate and subsequently decreasing in the unwanted oxide layer heterogeneity [9, 10].

2. Materials and procedures

The materials used to prepare and surface modification of NiTi alloys in this work are demonstrated in Table 1 with average sizes of particles, purity and origin of ingredients.

Table 1. List of powders , purity and particle size of the powders.

Material	Purity %	average sizes of particles (μm)	Source
Nickel powder	99.65	36.80	Changxing galaxy
Titanium powder	99.75	12.06	international Trade CO., LTD

Materials powders with (55wt % Ni and 45 % Ti) were weighted by using sensitive balance calibrated sensitive balance type (L220 S–D) with (Z 0.0001 % accuracy), German made. The powders were mixed in electric rolling mixer. Alumina balls with various diameters were utilized for mixing and refining the metal powder for six hours. Compacting process includes powders compacting of each samples via a die made from a high alloy steel with diameter of 14 mm (4g for each sample) as shown in Fig. 1 by using hydraulic presser type (4387-4NE0000,Carver) . The powder was pressed under pressure of 600 MPa. Then samples with 14 mm diameter and 4 mm height were produced.

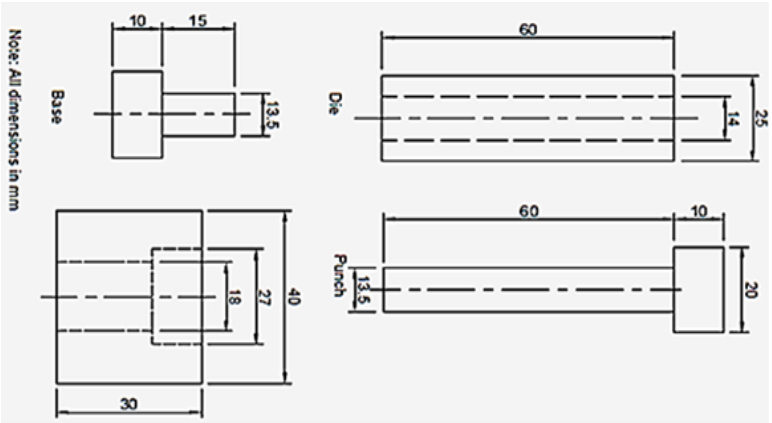

Figure 1. Compaction die.

The green compacted samples were sintered by using high temperature vacuum tube furnace, (model GSL 1600X, China) according to the program as shown in Fig. 2 . The pressure of the vacuum furnace was 10^{-4}torr. When the sintering program finished the samples were left inside the furnace to cool down till the temperature of sintered samples drops to room temperature.

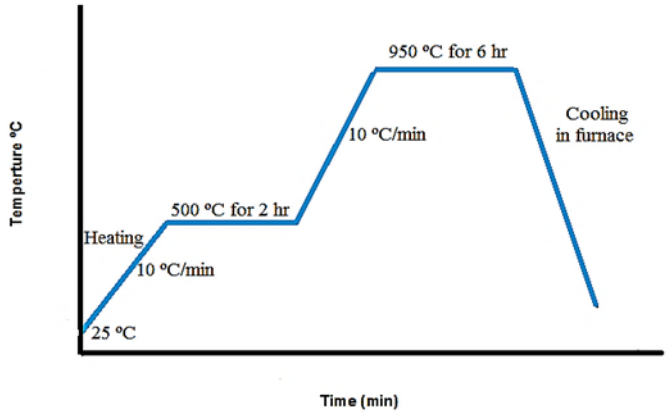

Figure 2. Sintering program of compacted sample.

The whole sample surfaces were wet ground utilizing 120, 220, 320, 600, 1000, 1200 and 2000, grit silicon carbide papers. Diamond paste of 6 µm was used to polish the samples to get a bright mirror finishing that is ready for the final step. Then these samples were degreased with acetone. After drying the samples, they were stored inside zip-lock plastic bags. Samples dimensions were measured and recorded. Etching of samples was achieved in solution with ingredients as follows [11]:
i- HF (10 ml) ,ii- HNO_3(20ml) and iii- H_2O (30ml).
The prepared samples were immersed for 15 seconds in etching solution, then washed with distilled water and dried, finally samples were ready for microstructure observations.

2.1. Surface modification processes
The sintered samples have been divided into two groups as shown in Table 2 .

Table 2. Samples coding.

Sample code	Descriptions of the samples
A	Bare NiTi (without surface modifications)
B	NiTi oxidized in aqueous solution containing 10%H_2O_2 at 60 °C

In this process the prepared samples were soaked in 10%H_2O_2 at 60 °C for 24 hours . Then, samples were left in a hot water at 60 °C for 72 hours and subsequently the oxidized samples were ultrasonically rinsed with deionized water for 10 min and dried in air at room temperature. This sample was B sample. The procedure was achieved according to Y.S. Dong [12]. Oxidation film thickness has been measured by using the cross-section of oxidized sample. The samples were placed in a cold-setting epoxy. Sequential grinding was performed starting from the finer silicon carbide paper (220) to the (1200) grit. Polishing was then conducted utilizing alumina suspension sequentially; the morphology of the coating and the cross section were examined via light optical microscope (Electron Eyepiece, model YJEYE01, resolution of 1280 (H)* 1024(V), Japan).

2.2. Tests
The sizes of the Ni and Ti particles were measured via (Laser particle size analyzer, Better size 2000, China). Phase's analysis of prepared sample is based upon X-ray diffraction technique and microstructure examination using optical electron microscope. X-Ray diffraction method is utilized to define the phases of bare samples (without coating) after sintering and for the sample after surface

modification. The x-ray generator with cu target, wavelength of 1.54060 Aº at 40 KV and 30 mA and speed of scanning equals to7º per minute (deg/min), respectively. The scanning range was (30º-90º). The microstructure of the base (NiTi) alloy and surface morphologies of samples after modifications were observed by optical microscopy type (Tescan Vega III China made) and Scanning Electron Microscopy (SEM) model FEI Quanta 450, Czech. The elemental composition of the base sample and surface modified layer was measured by EDS equipped with scanning electron microscopy. Potentiodynamic polarization technique in (0.5, 1, 1.5, 2) wt% NaF solution was used to test the samples corrosion behavior at room temperature with 1.76 cm^2 area. The following procedures were conducted:

1. After mounting the samples, grinding and polishing were conducted. Each sample was grinded with SiC emery paper in different grits starting from 600,800, 1000 grit to get flat and scratch free surface. Finally, these samples were polished with diamond paste of 6 µm to get a bright mirror finishing for the final step.
2. OCP (open circuit potential) of each sample was calculated in the four different solutions. The open circuit potential measurement was maintained up to (10) minutes with reading every 10 second. Corrosion rate measurement was obtained by applying the following equation [4].

$$\text{corrosion rate (mpy)} = 0.13 i_{corr}(E.W.)/A.\rho \quad (1)$$

Where; E. W. = equivalent weight (g/ eq), A = area (cm^2), density (g/ cm^3) = ρ (after sintering), 0.13 = metric and time conversion factor, and icorr. = current density (µA / cm^2).
The improvement (I%) was calculated from polarization curves using Eqn. 2 below, [4]:

$$I\% = (CR0 \_ CR / CR0)^x 100 \quad (2)$$

Where; CR° =the corrosion rate of base sample(without oxidation), CR =the corrosion rate of oxidized sample (after chemical oxidation),

3. Results and discussion

3.1. Particle size analysis

Fig. 3 and Fig. 4 show the results obtained from the analysis of particle size of Ni and Ti powders. The average sizes of Ti and Ni were about 12.06 µm and 36.80 µm, respectively. For getting good compactness and properties of final sintered products, various ranges of particle size are preferred [13].

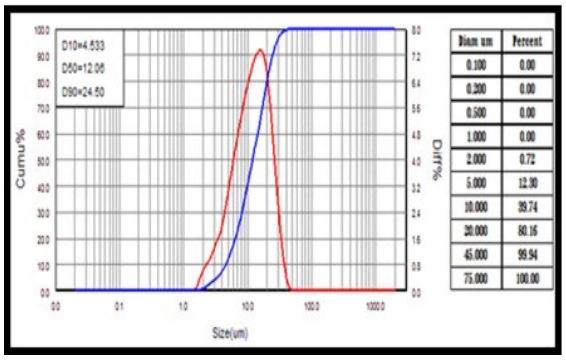

Figure 3. Distribution of Ti particle size.

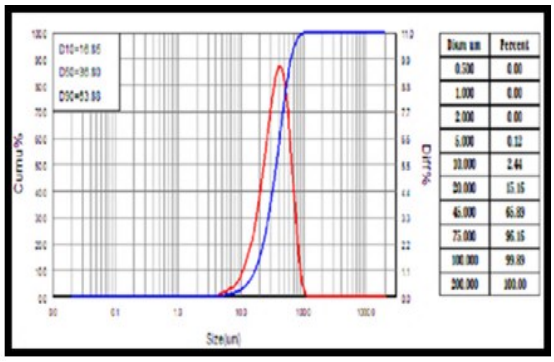

Figure 4. Distribution of Ni particle size.

3.2. XRD patterns

After preparing the samples, XRD test was conducted after sintering. Fig. 5 shows the diffraction patterns of sample compacted at 600 MPa after sintering process.

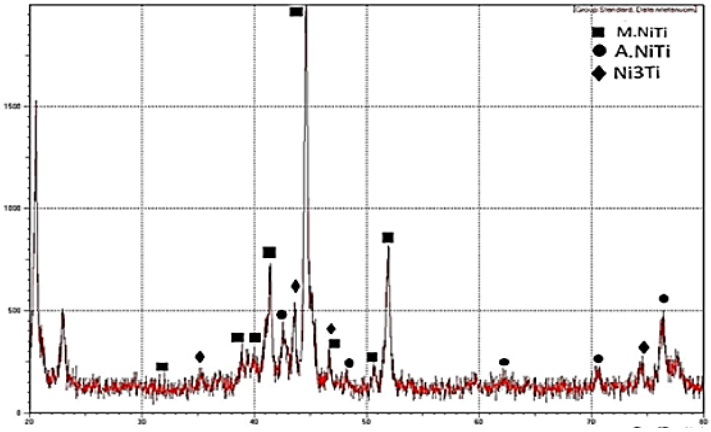

Figure 5. XRD pattern of sample compacted at 600 MPa after sintering process.

XRD technique was used to study the phases produced by the sintering process. Fig. 5 shows that there are almost certainly no pure metals appearance which proves that the temperature and time of sintering that were utilized in this study result in completed sintering reaction. Moreover, the samples compacted at 600 MPa consist principally of two phases; the martensitic phase (monoclinic B19′) and the austenitic phase (cubic B2), in addition to Ni_3Ti. The formation of Ni_3Ti might be ascribed to the samples' slow cooling inside the furnace. The suggested reactions throughout the process are as follows [4].

$$Ni + Ti \rightarrow NiTi \quad \Delta G: -67\ KJ / mol \tag{3}$$

$$Ni + Ti \rightarrow Ni_3Ti \quad \Delta G: -140\ KJ / mol \tag{4}$$

In accordance with the binary phase diagram of NiTi system, the NiTi and Ni_3Ti compounds are considered stable and reaction (4) is thermodynamically more preferable than reaction (3). Moreover, Fig. 5 indicates the absence of any oxides due to using the controlled vacuum atmosphere throughout the sintering process. The XRD patterns after oxidation in 10% H_2O_2 solution and water aging, Fig. 6 indicates the formation of TiO2 on the surface of samples in both anatase and routile forms and NiTi and Ni_3Ti phases. The absence of Ni oxide is because it is not thermodynamically favorable [12, 13].

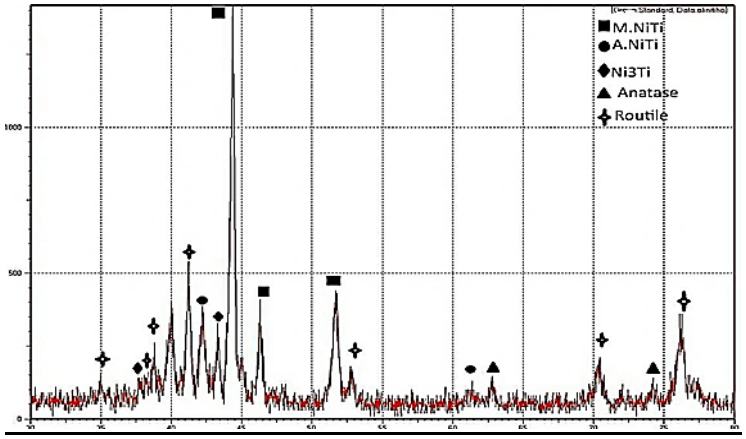

Figure 6. X-Ray diffraction of samples treated with 10% H_2O_2 at 60 C for 24 hours.

3.3. Microstructure observation

Fig. 7 shows the optical microscopy image of bare sample. This image shows some surface features such as grain boundaries, the open pores, and the NiTi and Ni_3Ti phases as well.

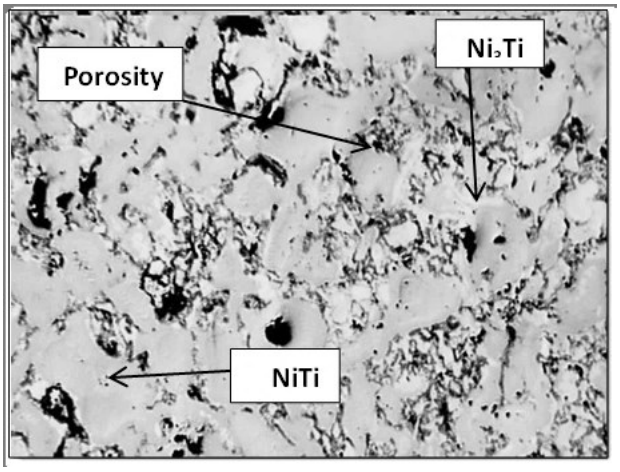

Figure 7. Optical microscope of NiTi sample after sintering process (200 X).

Fig. 8 shows across-section of NiTi SMA after chemical oxidation. The oxide layer of NiTi SMA is a continuous layer without any cracks which indicates that the layers are protective [14]. Also, Fig. 8 demonstrates the thickness of the oxide scale is about 42μm .

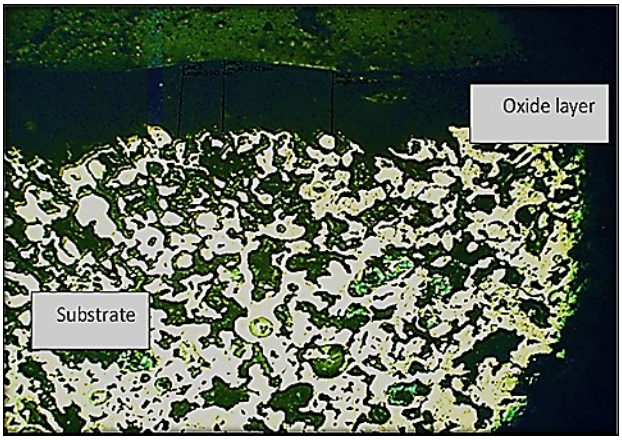

Figure 8. Cross section image of LOM of NiTi alloy after chemical oxidation in 10%H_2O_2.

SEM images of etched samples are shown in Fig. 9, while the EDS spectra are shown in Fig. 10.

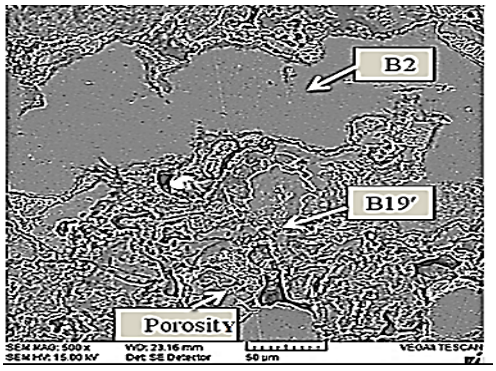

Figure 9. SEM image of NiTi bare sample

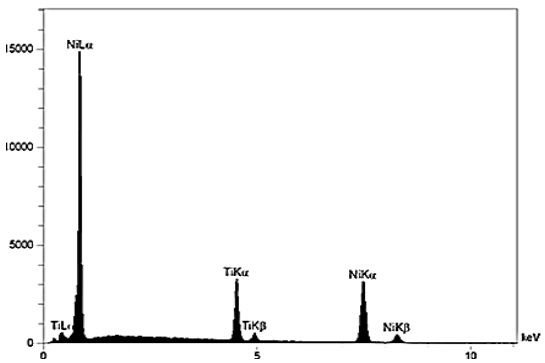

Figure 10. EDS spectra of NiTi bare sample

SEM images are very sensitive to the chemical composition. The sintered samples microstructure showed a multiphase structure in which the two phases (B2 - NiTi and Ni_3Ti) are embedded in uniformly gray matrix (NiTi-monoclinic phase B19′), thus, confirming XRD results [15, 16]. These results are supported by the expected phases found in the NiTi phase diagram. The result of EDS analysis for NiTi sample is shown in Fig. 10 showing the presence of Ni and Ti as base alloy. Table 3 lists the EDS analysis results. The EDS analysis results were fairly close to the addition percentages as the EDS analysis did not cover the total area but rather only the spot where the electron strokes. Furthermore, the EDS results assist in verifying the initial elemental purity of powders along with contamination prevention during casting and production of alloys [17].

Table 3. The result of EDS analysis for NiTi sample.

Element	Series	unn. C [wt.-%]	Norm [wt.-%]	Atom. C [at.-%]
Ti	K series	33.79	42.72	47.76
Ni	K series	45.32	57.28	52.24
		Total: 79.1 %		

Fig. 11a and Fig. 11b show SEM micrographs of NiTi bare sample and NiTi sample after chemical oxidations. As it can be seen from Fig. 11 b, the TiO_2 coating grown over the substrate did create an intermediate surface. The thickness of coating shown in Fig. 8 is approximately equal to 42μm. The TiO_2 coating crystallographic properties grown over NiTi alloys with chemical oxidation method were determined via XRD spectra given in Fig. 6. TiO_2 has the most common form of stable rutile and metastable anatase phases. Rutile and anatase are forms which usually coexist with the oxidation of titanium-containing compounds [12]. When crystallographic properties of TiO_2 coating grown over NiTi alloys with chemical oxidations method were observed from the XRD graphics given in Fig. 6. It was found that the coating contained predominantly rutile TiO_2 and anatase TiO_2. Additional crystalline phase obtained from XRD graphics is the phase from the NiTi base material. This situation shows that the achieved coating is very dense and smooth. These results are similar to [14,18].

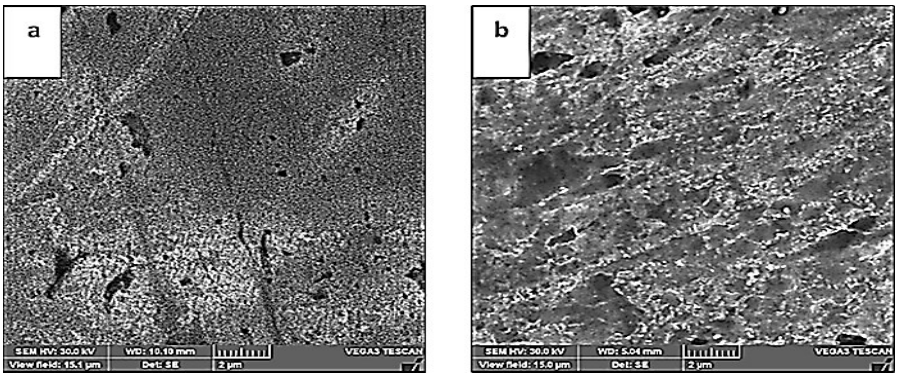

Figure 11. SEM micrographs of the : (a) Bare NiTi alloy and (b) NiTi alloy after chemical oxidation.

3.4. Corrosion test

The parameters of corrosion of all samples were calculated from the Potentiodynamic polarization test in all concentrations (0.5,1,1.5,2) wt % of NaF solution. The polarization curve of samples before and after the surface modification are shown in Fig. 12 and Fig. 13, respectively. Table 4 presents the corrosion parameters (corrosion potential and corrosion current density) of the samples before and after chemical oxidation. Clearly, there is an improvement in corrosion behavior of group B samples after the surface modification more than that of group A (before surface modification). The reasons may be related to the oxide layer (TiO2) which improves the corrosion resistance by good adherence of the oxide layer to the substrate [19]. These adherent and protective layers represent a barrier that isolates the alloy from its surrounding leading to shifting corrosion current resistance into lower values

and corrosion potential into higher values [(20, 21] as shown in Table 4. It is clear from Fig. 12 , Fig. 13 and Table 4 that the corrosion current of the blank and oxidized samples increased with increased concentration of NaF solution because of the presence of large number of harmful negative ions (F^-) in the solution [22] .

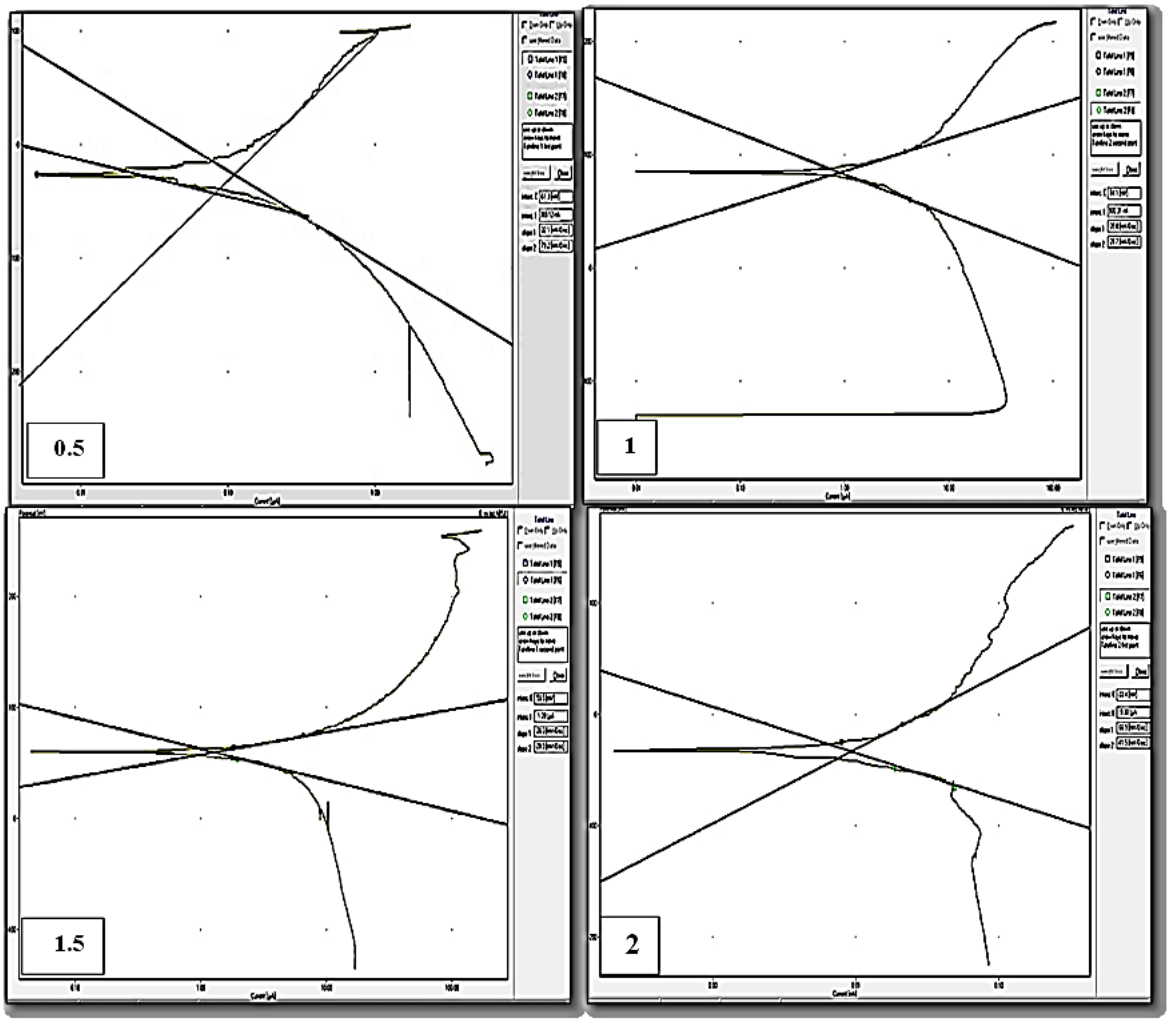

Figure 12. The polarisation curves of bare NiTi samples in different concentration (0.5, 1,1.5 &2) wt.% NaF solution.

Table 4. Corrosion parameters of all group samples in different concentration of NaF solutions.

Sample code	Concentration of NaF (wt%)	ICorr. $\mu A/Cm^2$	ECorr. mV	Corrosion Rate(mpy)	-bc mv/Dec	ba mv/Dec	I%
A1	0.5	0.303	-61.3	0.121	79.2	32.1	/
A2	1	0.900	84.1	0.359	35.8	28.7	/
A3	1.5	1.2	59.5	0.480	28	20	/
A4	2	9.30	-33.4	3.720	41.5	66.9	/
B1	0.5	0.074	140	0.028	51.8	68.5	76.8
B2	1	0.084	62.2	0.033	48.7	24.4	90.8
B3	1.5	0.137	47.5	0.0548	85.	74.6	88.7
B4	2	0.271	75.1	0.1084	93.8	89.3	97.8

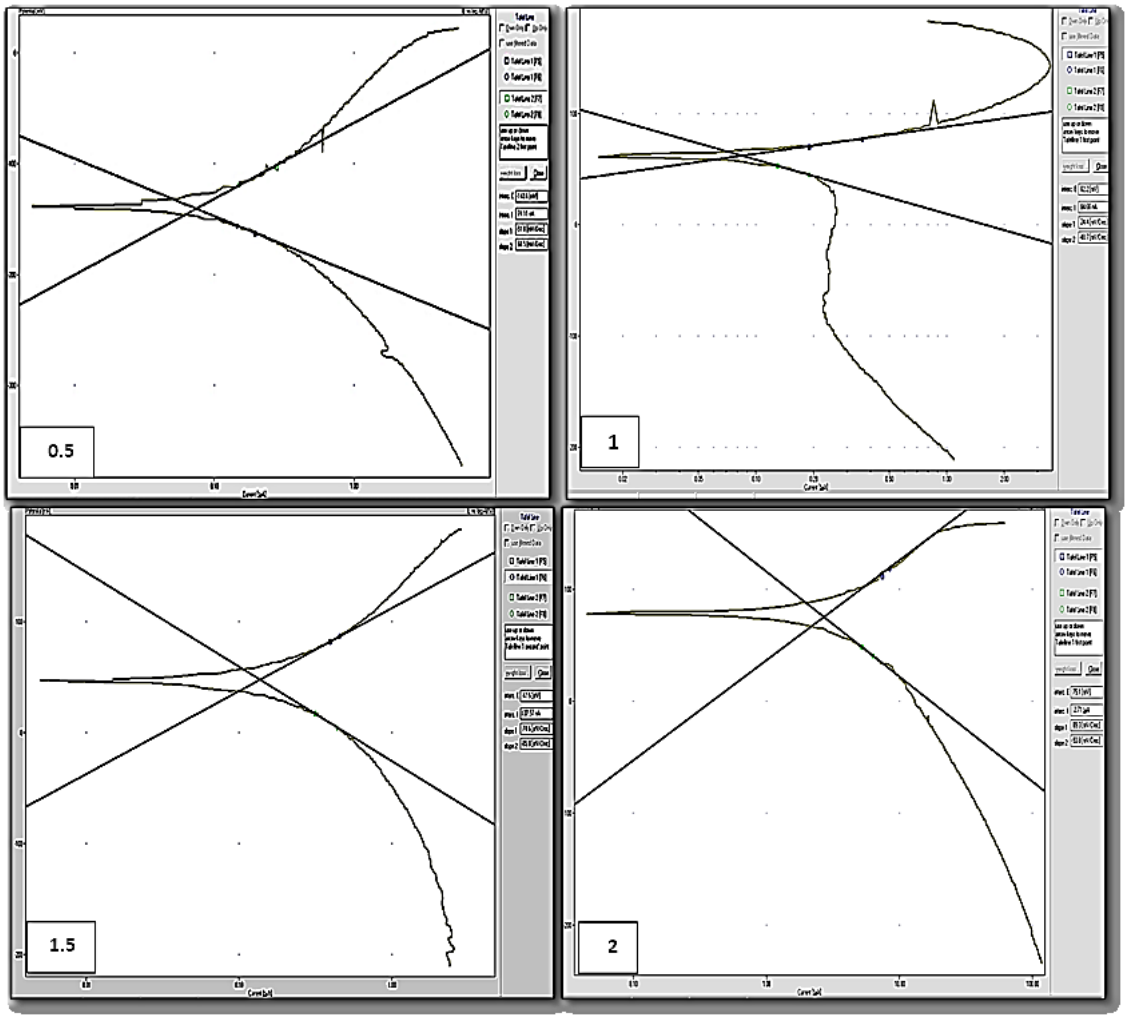

Figure 13. The polarisation curves of NiTi samples after chemical oxidation in different concentration (0.5, 1,1.5 &2) Wt% NaF solution.

4. Conclusions

Sample sintering at 950°C for 6 hours is efficient to obtain complete sintering and transform Ni and Ti into alloy structure. All samples (cooled inside the furnace) compacted at 600 MPa and sintered at 950°C for 6 hours gave a three-phase structure (NiTi cubic phase, NiTi monoclinic phase, and hexagonal Ni_3Ti phase) at room temperature. TiO_2 layer was formed on the samples surface treated with 10% H_2O_2 solution. It is clear that the oxide layer on NiTi SMA is a continuous layer without any cracks which indicates that the layer is protective.

5. References

[1] J Ryhnen, A Leminen and T Jams 2006 *A Novel Treatment of Grade III Acromielaviscular Joint Dislocations with a c-Hook Implant* (Arch Orthop Trauma Surg) vol 126 pp 22-27

[2] E Zanaboni 2008 *One Way and Two Way–Shape Memory Effects: Thermo Mechanical Characterization of Ni–Ti Wires* (M.Sc. Thesis, Biomedical Engineering Department, Pavia University)

[3] E Patoor, D C Lagoudas and P B Entcheve 2006 *Shape Memory Alloys, Part I: General Properties and Modeling of Single Crystals* (Mechanics of Materials) vol 38 pp 391-429

[4] Z J Ridha 2016 *Preparation and Studying Properties of NiTi SMA Coated with Biocompatible Layer* (M.Sc. Thesis, Material Engineering, University of Babylon)

[5] G Olender, R Pfelfer and C W Muller 2011 *A Preliminary Study of Bending Stiffness Alteration*

in Shape Changing Nitinol Plates for Fracture Fixation (Biomedical Engineering) vol 39 no 5 pp 1546-1554

[6] S Lombard and P Poncet 2005 *Metallurgical Principles of Nitinol and Its Use in Interventional Device* (Any Key Words: Nitinol, Shape Memory, Superelasticity, Medical Device)

[7] Lagoudas, Dimities C 2008 *Shape Memory Alloys Modeling and Engineering Application* (Texas AZM University, USA)

[8] S L Angionic, M Meo and A Foreman 2011 *Impact Damage Resistance and Damage Suppression Properties of Shape Memory Alloys in Hybrid Composites-a Previous* (Smart Mater Strut) vol 20 pp 1–24

[9] T Yoneygma and S Miyazaki 2009 *Shape Memory Alloys for Biomedical Application* (Cam Bridge, England)

[10] A Biscarini, G Mazola and A Tuissi 2008 *Enhanced Nitinol Properties for Biomedical Application* (Biomedical Engineering) vol 1 no 3 pp 180-196

[11] S Dilibal, H Adanir *2013 Comparison and Characterization of NiTi and NiTiCu Shape Memory Alloys* (Marmara University, Istanbul/Turkey)

[12] Y S Dong, C Guo and J C Y Chung 2007 *In Vitro Biocompatibility of Titanium–Nickel Alloy with Titanium Oxide Film by H2O2 Oxidation* (Transactions of Nonferrous Metals Society of China) vol 17 no 3 pp 553-557

[13] M A Sadeq 2013 *Corrosion Behavior of Biocompatible Coatings of Porous NiTi Shape Memory Alloy* (Ph. D. Thesis, Production Engineering and Metallurgy Department, University of Technology)

[14] E E Sukuroglu, S Sukuroglu and K Akar 2017 *The Effect of TiO2 Coating on Biological NiTi Alloys After Micro-Arc Oxidation Treatment for Corrosion Resistance* (Proceedings of the Institution of Mechanical Engineers, Part H: Journal of Engineering in Medicine)

[15] D Qiua, A Wanga, Y Yinb 2010 *Characterization and Corrosion Behavior of Hydroxyapatite/Zirconia Composite Coating on NiTi Fabricated by Electrochemical Deposition* (Applied Surface Science) vol 257 no 5 pp1774–1774

[16] N M Dawod, A R Kadhum and A A Atiyah 2019 Fabrication of Porous NiTi Shape Memory Alloy Objects by Powder Metallurgy for Biomedical Applications (IOP Conf. Series: Materials Science and Engineering) vol 518

[17] N M Dawood 2020 Erosion-Corrosion Behavior of Al-20%Ni-Al2O3Metal Matrix Composites by Stir Casting (Materials Science Forum) vol 1002 pp 161-174

[18] P Gill, V Musaramthota, N Munroe, A Datye, R Dua, W Haider, A McGoron and R Rokicki 2015 *Surface Modification of Ni–Ti Alloys for Stent Application After Magnetoelectropolishing* (Materials Science and Engineering C) vol 50 pp 37-44

[19] C L Chua, C Y Chungb and P K Chub 2006 Surface *Oxidation* of NiTi *Shape Memory Alloy* in a *Boiling Aqueous Solution Containing Hydrogen Peroxide* (Materials Science and Engineering A) vol 417 pp 104–109

[20] M F Chen, X J Yang, Y Liu, S L Zhu, Z D Cui and H C Man 2003 *Study on the Formation of an Apatite Layer on NiTi Shape Memory Alloy Using a Chemical Treatment Method* (Surface and Coatings Technology) vol 173 pp 229–234

[21] S Chao, Xiao-bo, L Ping-hua and C Paul K 2009 *Surface Treatment of NiTi Shape Memory Alloy by Modified Advanced Oxidation Process* (Trans. Nonferrous Met. Soc. China) vol 19 pp 575-580

[22] X Li, J Wang and E H Han 2007 Influence of Fluoride and Chloride on Corrosion Behavior of NiTi Orthodontic Wires (Acta Biomaterial) vol 3 pp 807-815